KSME Journal, Vol. 7, No. 4, pp. 312~319, 1993

Flow Analysis of Engine Cooling System for a Passenger Vehicle

Jongsoo Jurng*, Nahmkeon Hur*, Kwang Ho Kim* and Chun Sik Lee*

(*Received February 15, 1993*)

A numerical simulation is carried out to analyze the flow field of cooling air through the radiator and engine compartment. In order to consider the strong effect of the suction-type flow by the cooling fan at engine idling condition, a potential flow analysis is attempted by the assumption of a line sink located at the position of the cooling fan. The governing equations for steady two-dimensional, incompressible, turbulent flow are solved with the two-equation k-ε model for turbulence. The velocity profiles in the underhood engine compartment and around the front-end of a real vehicle are measured to compare with the numerical results. The agreement between the numerical and experimental results is fairly good. It is concluded that a two-dimensional computation is a fast and efficient tool for predicting the effect of front-end design on the cooling air flow through the radiator.

Key Words: Cooling Air Flow, Front-End Shape, Potential Flow Analysis, Schwarz-Christoffel Transformation

Nomenclature

D_{fan} : Depth of the volume swept by the cooling fan
D_{ha} : Hydraulic diameter of the cooling air passage
f : Friction factor
F : Function of complex variables
h, h' : Geometrical parameters (Fig. 1)
ΔP_o : Pressure change through the fan
Q : Volume flow-rate for line sink
S : Momentum source term
u_{fan} : Air velocity at fan location in x direction
u_{rad} : Cooling air velocity through the radiator
u, v : Velocity components in x and y direction, respectively
W : Complex velocity
α_p : Gradient of pressure change through the fan
ρ : Density of air
μ_{eff} : Effective viscosity
Φ : Velocity potential
ζ : Complex variable

* Thermal/Fluids Engineering Lab., Korea Institute of Science and Technology, Seoul 130-010 Korea

1. Introduction

The shape of the front-end of a passenger vehicle greatly affects the aerodynamic performance of a vehicle as well as the cooling performance of an engine. The external shape of a vehicle is usually determined based on considering both the vehicle aerodynamics and styling. When an engine is laid out in a vehicle, the problems of the insufficient cooling performance can be found. This is because of the insufficient cooling air flowing through the radiator and around the engine. This usually requires the design modifications consuming cost and time. Therefore the cooling performance of the engine should be analyzed in the early design stages. However, the drag of a vehicle increases as the flow rate of the cooling air entering into the engine compartment increases. This is mainly due to the high resistance against the flow through the engine compartment. An optimal design is required in view of both vehicle aerodynamics and

engine cooling performance. One can find many studies from the literature on engine cooling performance from the aerodynamic point of view (e.g., Williams, 1985 ; Garrone and Masoero, 1986 ; Shibata et al., 1990, among others).

In order to predict the performance of the engine cooling system of a vehicle, the automotive engineer must analyze the flow through engine compartment. This is because the flow rate through the radiator affects the heat rejection from it. The flow field around the engine also affects the cooling air flow. The flow passages in the engine compartment are being obstructed by many engine components such as the condenser of automotive air-conditioner, radiator, oil cooler, cooling fan, engine, and air cleaner, etc. The flow also passes the bumper, radiator grille, air dam and license plate, and enters into the engine compartment, which makes the flow field more complicated.

Willoughby et al.(1985) have performed a quasi-three-dimensional computation for flow through engine compartment by applying variable-cell-depth to two-dimensional computation. China and Kameyam(1988) also showed two-dimensional computational procedure to predict the air flow for engine cooling. Recently due to the developments of the high speed computers, Aoki et al.(1990) have performed numerical computation of three-dimensional flow by using a commercial software and showed that the cooling air-flow analysis can be employed in the early design stages.

In the present study, a two-dimensional computation is performed in order to study whether it can be applied to the three-dimensional actual flow situation. An efficient solving method is attempted for flow field at engine idling condition. Experiments are also performed in wind tunnel to compare the results with the numerical simulation.

2. Potential Flow Analysis

When an engine is in idling condition, the air flow for cooling is only induced by the cooling fan. In this case the flow through the radiator and around the front-end of a vehicle is generated by the suction of the cooling fan. This type of flow field can be solved by putting a momentum source and setting a pressure-boundary condition at the boundary of the computational domain. The momentum source is equivalent to the fan power at the volume swept by the cooling fan. This computation, however, usually requires much more CPU time to get convergence than boundary-specified case because the velocities are not specified at the boundary.

In order to overcome this problem, a new solution procedure has been attempted. The potential flow equations are solved by simplifying the geometry and assuming momentum sink at the position of the cooling fan to get the velocities at the boundary of the computational domain.

For the two-dimensional incompressible inviscid flow, the following Laplace equation can be obtained

$$\nabla^2 \Phi = 0, \tag{1}$$

where Φ is the velocity potential from which the velocity components can be obtained as follows :

$$u = \frac{\partial \Phi}{\partial x}, \quad v = \frac{\partial \Phi}{\partial y}. \tag{2}$$

In the present study the Schwarz-Christoffel transformation is used to map the physical domain into the imaginary computational domain (see Fig. 1). The transformation is as follows :

$$\frac{dz}{d\zeta} = k[\zeta(\zeta-1)]^{-1/2} \tag{3}$$

Integrating Eq. (3) along with the boundary condition gives

$$z = \frac{8}{\pi}(h'-h)\left[\frac{2\zeta-1}{4}(\zeta(\zeta-1))^{1/2} - \frac{1}{4}\ln((\zeta-1)^{1/2}+\zeta^{1/2})\right] + ih'. \tag{4}$$

Now the complex velocity W is defined as

$$W = U - iV = \frac{dF}{dz} = \frac{dF}{\partial\zeta}\frac{\partial\zeta}{dz}, \tag{5}$$

where $\frac{dF}{d\zeta}$ can be obtained by expressing line sink with volume flow rate Q as

$$\frac{dF}{d\zeta} = -\frac{Q}{\pi}\frac{1}{\zeta}. \tag{6}$$

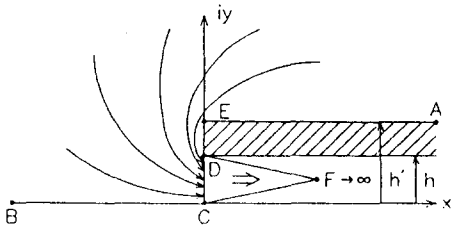

(a) z-plane

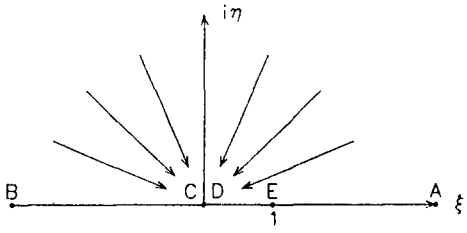

(b) ζ-plane

Fig. 1 Mapping planes of Schwarz-Christoffel transformation

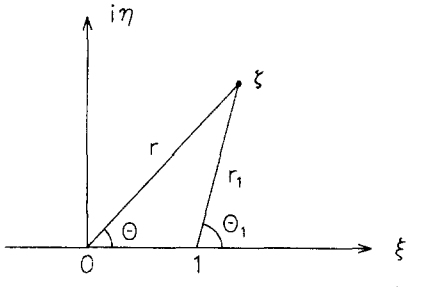

Fig. 2 Geometrical relationships in ζ-plane

Together with the following geometrical relationships (see Fig. 2)

$$\zeta = re^{i\theta},$$
$$\zeta - 1 = r_1 e^{i\theta_1}. \tag{7}$$

Equations (3) and (5) give the expression for the velocity components U and V as

$$U = -\frac{Q}{8}\frac{1}{(h'-h)r^{3/2}r_1^{1/2}}\cos\left(\frac{3}{2}\theta+\frac{1}{2}\theta_1\right), \tag{8}$$

$$V = -\frac{Q}{8}\frac{1}{(h'-h)r^{3/2}r_1^{1/2}}\sin\left(\frac{3}{2}\theta+\frac{1}{2}\theta_1\right). \tag{9}$$

Here x and y can also be expressed from Eq. (4) as follows:

$$x = \frac{2}{\pi}(h'-h)[2r^{3/2}r_1^{1/2}\cos\left(\frac{3}{2}\theta+\frac{1}{2}\theta_1\right) - (rr_1)^{1/2}\cos\left(\frac{1}{2}\theta+\frac{1}{2}\theta_1\right) - \ln(r)], \tag{10}$$

$$y = \frac{2}{\pi}(h'-h)[2r^{3/2}r_1^{1/2}\sin\left(\frac{3}{2}\theta+\frac{1}{2}\theta_1\right) - (rr_1)^{1/2}\sin\left(\frac{1}{2}\theta+\frac{1}{2}\theta_1\right) - \theta + h]. \tag{11}$$

The above four parametric equations can be solved to get the velocity (U, V) at the location (x, y). However, it is not an easy task to solve these equations analytically so that in the present study a numerical solution is obtained. Velocities at the boundaries are then used as boundary conditions for the viscous-flow computation at idling condition.

3. Numerical Analysis

The equations to be solved are steady, two dimensional, incompressible, turbulent flow equations as follows:

$$\frac{\partial}{\partial x}(\rho u)+\frac{\partial}{\partial y}(\rho v)=0, \tag{12}$$

$$\rho u\frac{\partial u}{\partial x}+\rho v\frac{\partial u}{\partial y} = \frac{\partial}{\partial x}(\mu_{eff}\frac{\partial u}{\partial x})+\frac{\partial}{\partial y}(\mu_{eff}\frac{\partial u}{\partial y})+S_u, \tag{13}$$

$$\rho u\frac{\partial v}{\partial x}+\rho v\frac{\partial v}{\partial y} = \frac{\partial}{\partial x}(\mu_{eff}\frac{\partial v}{\partial x})+\frac{\partial}{\partial y}(\mu_{eff}\frac{\partial v}{\partial y})+S_v, \tag{14}$$

where ρ is a density of air and u, v are the velocity components in x and y direction, respectively. μ_{eff} denotes the effective viscosity and contains the effects of turbulence, which are obtained by solving the standard equations for the turbulent kinetic energy and its dissipation rate employing a wall-function approach near the wall. Standard equations for the turbulent kinetic energy with inlet turbulent intensity level of 0.05 u^2 and its dissipation rate are used in the present study and can be found elsewhere.

S_u and S_v in the above equations are momentum source terms which are defined as follows:

$$S_u = \frac{\partial}{\partial y}(\mu_{eff}\frac{\partial u}{\partial x})+\frac{\partial}{\partial x}(\mu_{eff}\frac{\partial u}{\partial y})$$

$$-\frac{\partial P}{\partial x}+S_{hu}+S_{fu}, \tag{15}$$

$$S_v=\frac{\partial}{\partial x}(\mu_{eff}\frac{\partial v}{\partial y})+\frac{\partial}{\partial y}(\mu_{eff}\frac{\partial v}{\partial x})$$
$$-\frac{\partial P}{\partial y}+S_{hu}+S_{fu}, \tag{16}$$

where S_{hu} and S_{fu} are the momentum source terms due to the radiator and the cooling fan in x direction, respectively (S_{hv} and S_{fv} for y direction).

In the present study, the radiator and the fan are considered to be in vertical position so that S_{hv} and S_{fv} are zero everywhere. S_{hu} and S_{fu} are modeled based on the experiment (Jurng et al., 1990) as follows:

$$S_{hu}=\frac{f}{2}\rho u_{rad}^2\frac{4}{D_{ha}}, \tag{17}$$

$$S_{fu}=\frac{\Delta P_o}{D_{fan}}+\alpha_p\frac{u_{fan}}{D_{fan}}, \tag{18}$$

where f is the friction factor and u_{rad} is the cooling air velocity through the radiator. D_{ha} is the hydraulic diameter of the cooling air passage consisting of radiator fins and outer walls of the water tubes. The value of the friction factor f in the present study is obtained from Blasius solution, using Reynolds number based on the louver pitch of the fin (see Jurng et al., 1990, also Davenport, 1983, for detailed discussion). In Eq. (7), ΔP_o is the pressure change through the fan and α_p is the gradient of pressure change due to the change of air velocity. u_{fan} is the air velocity in x direction at fan location and D_{fan} is the depth of the volume swept by the cooling fan.

No-slip condition at the surfaces of both the vehicle and the road is used. Grid points of 55×60 are used to define the computational domain. A control-volume-based computation is performed with the staggered-grid system employing a power-law scheme for discretizing the convection terms and SIMPLE algorithm for the solution procedure using tri-diagonal matrix solver (TDMA). For a computation of one case, it takes approximately 2,000 seconds of CPU time for 1, 500 iterations using 32-bit workstation (Solbourne 5-501, 22 mips). The convergence is assured when the maximum error of the continuity equation at each control volume is less than 10^{-10}.

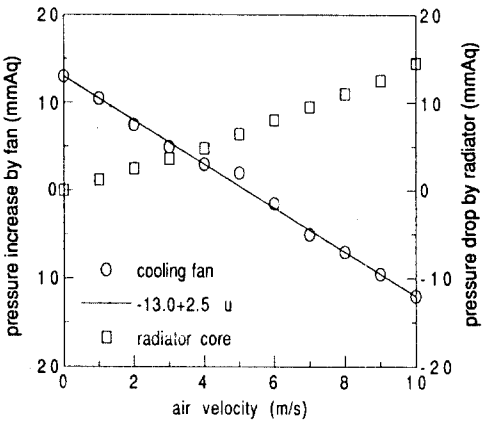

Fig. 3 Pressure increase by a cooling fan and pressure drop by radiator core(Jurng et al., 1990)

In the present study, $\Delta P_o=13$ mmAq and $\alpha_p=-2.5$ (mmAqs)/m are used based on the measured pressure drop of the radiator fan (Jurng et al., 1990). Figure 3 shows the measured pressure increase by fan and pressure drop by radiator with varying air velocity.

4. Experiments

In order to get the information of the complicated flow field and to compare with the computations, the experiments are performed. As well as the external flow around the front-end of the vehicle, the internal flow in the engine compartment are measured. When the engine is in idling condition, the flow field induced by the cooling fan has been measured. For simulating actual running condition, the experiments are performed by placing a vehicle in an environmental test chamber. This facility can simulate up to 200 km/h of vehicle speed.

The air velocity is measured using pitot tubes and micro-manometers (Furness Controls Ltd., Model FCO12-3) for the six incoming air velocities of 0, 20, 40, 60, 80 and 100 km/h. At each measurement, the directions of Pitot tubes are adjusted such that a maximum velocity can be measured at each point. The air velocities are measured simultaneously for the flow field at 20 measuring points inside the engine compartment,

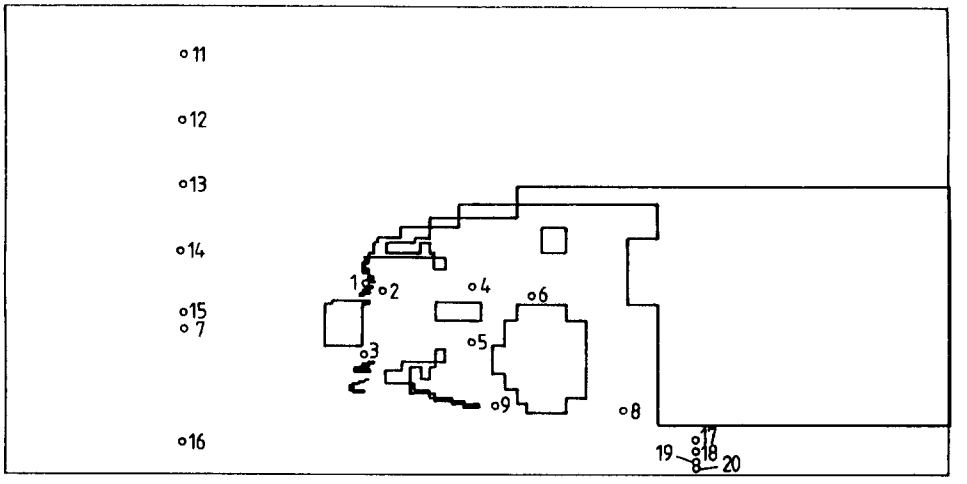

Fig. 4 Measuring points of air velocity in the center plane of a vehicle

around the front-end and underneath the vehicle.

Figure 4 shows the locations where the velocity measurements are taken along with the computational model of a vehicle front-end. The measuring points 7 and 11 through 16 are located 0.28 m in front of the bumper, points 17 through 20 being located 1 m from the front axle.

5. Results and Discussion

In Figs. 5, 6 and 7, comparisons between computations and measurements are made for the air velocities at various locations.

The air velocity through a radiator greatly affects the radiator performance. This is measured at point 2 in Fig. 4 (in front of the condenser) and shown in Fig. 5. When the vehicle speed is higher than 40 km/h, the cooling air velocity increases linearly proportional to the vehicle speed. Whereas, in the region of the vehicle speed lower than 40 km/h, the cooling air velocity is not proportional to the vehicle speed, because of the cooling fan flow. Comparison between computations and measurements shows a good agreement.

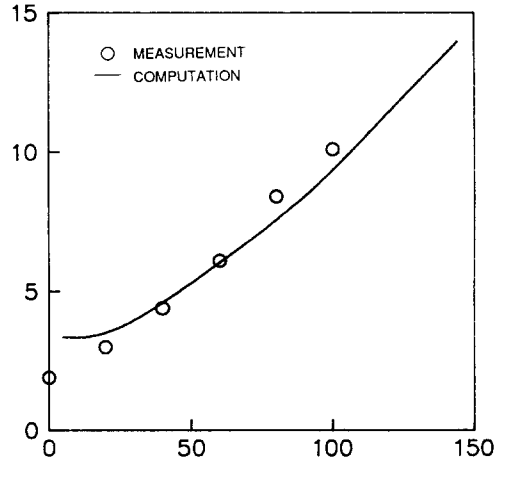

Fig. 5 Cooling air velocity in front of the condenser and radiator at various vehicle speed

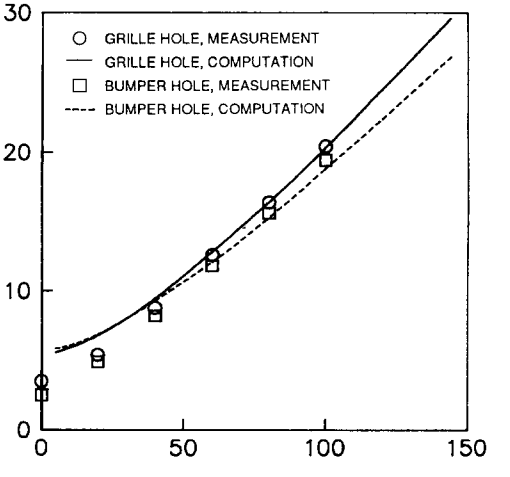

Fig. 6 Cooling air velocity at grille hole and bumper hole at various vehicle speed

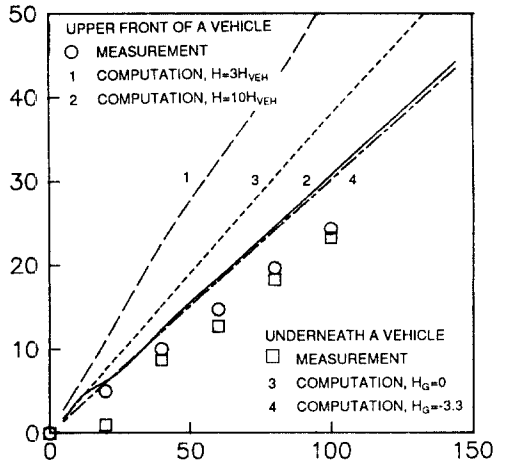

Fig. 7 Air velocity at upper front and under a vehicle at various vehicle speed

Figure 6 shows the velocities at the radiator-grille hole and the bumper hole (points 1 and 3 in Fig. 3, respectively). As shown in the figure, velocities at both locatioins increase linearly as the vehicle speed increases faster than 40 km/h. The effect of cooling fan is seen in the lower vehicle speed region, which has the same trend as in the velocities in front of the condenser. The velocity at radiator-grille hole is slightly higher than those at bumper hole. This may be because the grille hole is closer to the cooling fan. The agreement between computations and measurements is fairly good except in the range of vehicle speed closer to the idling condition.

The velocities at points 11 and 20 of Fig. 3 are compared in Fig. 7. Point 11 is located at 1.4 m above ground and 0.28 m in front of bumper, while point 20 is located 20 mm above ground and 1 m behind front axle.

In the measurements, these velocities increase linearly as vehicle speed increases. It is interesting that the measured velocities are almost the same at both locations, in front of and under a car. However, in the computation, air velocity under a car is larger than incoming air velocity. This discrepancy is mainly because of the effect of blockage ratio and three-dimensional flow. In two-dimensional computation, the blockage ratio (ratio of vehicle frontal area to the computational domain) is relatively high so that the computed velocities at these points are much bigger than the measured ones from the conservation of mass.

Line 1 of Fig. 7 represents the computed velocities at upper front of a vehicle when the height of the computational domain is three times as high as the height of a vehicle. Whereas in line 2, the computational domain is 10 times as high as the height of a vehicle. One can clearly see the effect of blockage ratio from the figure. In the limit of zero blockage ratio, the velocities at these points

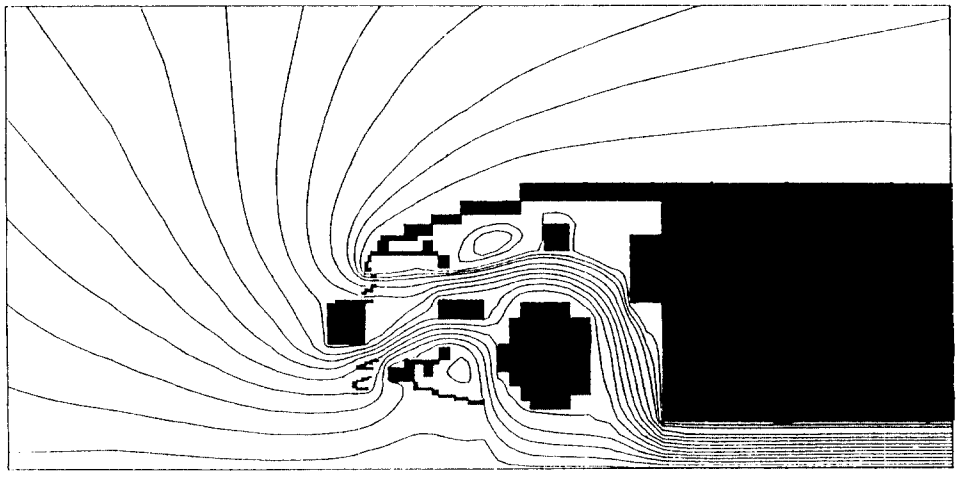

Fig. 8 Computed streamlines showing flow around front-end of a vehicle and inside engine compartment at idling condition

approach the vehicle speed.

The computed air velocity at 2 mm above the ground is denoted by line 3 of Fig. 7. Line 4 represents the same when the ground is located 3. 3 m below the vehicle. These lines also show the effect of blockage ratio. However, the blockage ratio has little effect on the flow inside an engine compartment, especially on the cooling air velocity through radiator.

Figure 8 shows the computed streamlines at idling condition. Here, the air velocities at boundary are obtained from the potential-flow analysis as mentioned earlier. In the figure, the flow-recirculation regions can be seen, which usually cause a pressure loss and a heat build-up in important components.

By comparing the air velocities inside the engine compartment (especially around the engine block), there are some discrepancies between the computed and measured velocities. This is due to the three-dimensionality of the flow inside engine compartment. Therefore, a two-dimensional computation could not be an excellent tool for predicting the three-dimensional flow field inside engine compartment accurately.

However, this two-dimensional computation with a potential analysis can be a fast and efficient tool if an automotive engineer wants to predict only the radiator performance of a particular car by calculating the amount of the cooling air flow through the radiator.

6. Concluding Remarks

A numerical computation for the steady two-dimensional incompressible turbulent flow has been performed for the air flow around the front-end and inside the engine compartment of a vehicle. The air velocities are also measured in order to compare with the computation.

In idling condition, a new method of getting boundary conditions by solving a potential flow equation has been attempted. It is anticipated that this method can be improved to give more accurate boundary conditions and initial conditions and hence to give faster convergence of the viscous flow solver in complicated geometries. Good agreements have been obtained overall. However, there were some discrepancies at some measuring points between the measured and computed results. It is because the two-dimensional flow field is assumed for the three-dimensional actual flow situation. The two-dimensional computation could not be an excellent tool for predicting the three-dimensional flow field inside engine compartment accurately. However, it can be a fast and efficient tool for predicting the flow rate of the cooling air through the radiator, compared with the time-consuming three-dimensional computation. This method, in turn, can be used to predict the performance of the radiator.

Further studies are recommended to improve the models for the momentum source terms induced by the radiator and the cooling fan. The incorporation of energy equation is also needed to solve the temperature field and hence to predict the performance of the radiator.

References

Aoki, K., Hanaoka, Y. and Hara, M., 1990, "Numerical Simulation of Three Dimensional Engine Compartment Air Flow in FWD Vehicles," SAE Paper 900086.

China, H. and Kameyama, J., 1988, "A Two Dimensional Computational Procedure for Prediction of Engine Cooling Air Flow," JSAE Review, Vol. 9, No. 2, pp. 94~95.

Davenport, C.J., 1983, "Correlations for Heat Transfer and flow friction characteristics of louvered fin," AIChE Symposium Series, V. 79, No. 225, pp. 19~27.

Garrone, A. and Masoero, M., 1986, "Car Underside, Upperbody and Engine Cooling System Interactions and Their Contributions to Aerodynamic Drag," SAE Paper 860212.

Jurng, J., Hur, N., Kim, K.H. and Lee, C.S., 1991, "Analysis of Engine Cooling System for a Passenger Vehicle," Proceedings of the Sixth International Pacific Conference on Automotive Engineering (IPC-6), Paper 912525, pp. 437~443.

Jurng, J., Kim, K.H. and Lee, C.S., 1990, "A Study on the Analysis of the Engine Cooling Performance for Various Front-End Shapes,"

MOST Report BSI-1316-3791-2.

Jurng, J. and Lee, C.S., 1989, "Design of the Heat Dissipation Rate of Automotive Raiators-(1) Analysis of Heat Dissipation," Journal of Korea Society of Automotive Engineers, V. 11, No. 5, pp. 65~75.

Lee, C. S., Kim, Y. I., Kim, K. H. and Jurng, J., 1987, "A Design Technology for Automotive Radiator with Optimal Heat Dissipation Performance for Various Engine Types," MOST Report N288-2929-2, KIST.

Shibata, Y., Hosoka, S., Fujitani, K. and Himeno, R., 1990, "A Numerical Analysis Method for Optimizing Intercooler Design in the Vehicle Development Process," SAE Paper 900080.

Williams, J., 1985, "An Automotive Front-End Design Approach foir Improved Aerodynamics and Cooling," SAE Paper 850281.

Willoughby, D. A., Garol, G. W., Sun, R. L., Wiliams, J. and Maxwell, T.T., 1985, "A Quasi 3-D Computational Procedure for Prediction of Turbulent Flow through the Front-End of Vehicles," SAE Paper 850282.